GEORGIAN MEDICAL NEWS

ISSN 1512-0112

NO 5 (362) May 2025

TBILISI - NEW YORK

MONTHLY SCIENTIFIC JOURNAL
Georgian Medical News
საქართველოს სამედიცინო სიახლენი

MORPHOMETRIC THRESHOLDS OF THE OSTIOMEATAL COMPLEX AND THEIR PSYCHOLOGICAL CORRELATES IN SINUS VENTILATION IMPAIRMENT

Yurevych N.O[1], Kysylenko K.V[1], Sukhina I.S[1], Falova O.Ye[2], Khartsiy O.M[2], Rozhkova O.Y[3], Lupyr M.V[1], Alekseeva V.V[1,4]*

[1]*Kharkiv National Medical University, Kharkiv, Ukraine.*
[2]*V. Karazin Kharkiv National University Kharkiv, Ukraine.*
[3]*Kyiv Medical University, Kyiv, Ukraine.*
[4]*Kharkiv International Medical University, Kharkiv, Ukraine.*

Abstract.

Background: The ostiomeatal complex (OMC) is a critical anatomical region ensuring ventilation and drainage of the anterior paranasal sinuses. Variability in its morphology can lead to functional impairment and predispose individuals to chronic rhinosinusitis.

Objective: To determine quantitative morphomet
ric thresholds associated with inadequate sinus ventilation based on OMC structure and semilunar hiatus dimensions using CT data and computational modeling.

Methods: Morphometric analysis was performed on 400 spiral CT scans. OMC parameters were measured manually and automatically, and 3D models were constructed. Pressure and flow simulations were conducted using the IMED system. Subjects were divided into three groups based on the width of the semilunar hiatus: narrow, moderate, and wide. Parameters such as sinus wall thickness, OMC component density, and estimated ventilation pressure were analyzed.

Results: Both excessively narrow (<1.8 mm) and overly wide (>3.5 mm) semilunar hiatuses were associated with impaired ventilation. Optimal airflow occurred in the intermediate range (2.1–3.2 mm). A pressure gradient of <2.5 Pa between the maxillary sinus and nasal cavity was associated with stasis in 73% of cases. Strong correlations were observed between sinus ventilation efficiency and the thickness of the uncinate process ($r = -0.75$, $p < 0.01$), as well as medial maxillary sinus wall thickness ($r = -0.72$, $p < 0.05$).

Conclusion: Functional ventilation of the maxillary sinus requires a semilunar hiatus width between 2.1 and 3.2 mm and a pressure differential above 2.5 Pa. Both morphological extremes are associated with physiological dysfunction, highlighting the importance of patient-specific anatomical assessment in surgical planning.

Key words. Computer tomography, paranasal sinusis, ostiomeatal complex, anatomy, 3D model.

Introduction.

The ostiomeatal complex (OMC) is the central conduit for drainage and ventilation of the anterior paranasal sinuses, particularly the maxillary, frontal, and anterior ethmoid sinuses. Its functional integrity is essential for maintaining normal mucociliary clearance and pressure regulation within these sinuses [1,2]. As a key anatomical structure, the OMC encompasses several interrelated components: the uncinate process, ethmoid infundibulum, semilunar hiatus, middle meatus, and associated drainage pathways [3,4]. Disruption of this narrow anatomical corridor, whether from inflammation, anatomical variation, or iatrogenic alteration, is a well-established cause of chronic rhinosinusitis (CRS) [5,6].

Despite the clear clinical importance of the OMC, there remains significant uncertainty about the quantitative anatomical thresholds that define functional obstruction [7,8]. Much of the existing literature is descriptive, categorizing variants such as concha bullosa, Haller cells, and paradoxical middle turbinates, without linking these findings to specific functional impairments [9,10]. Similarly, while imaging plays a crucial role in preoperative assessment, radiological interpretations often rely on subjective criteria, such as "narrowing" or "opacification," rather than precise numerical values [11,12]. This gap between structural imaging and functional prediction is a major limitation in evidence-based surgical planning [2,13], in reconstructive dentistry [14,15].

Contemporary endoscopic sinus surgery (ESS) approaches the OMC with the intent of restoring drainage and ventilation, typically by enlarging the semilunar hiatus and removing anatomical obstructions such as the anterior ethmoid cells or hypertrophic uncinate process. However, postoperative failure and persistent symptoms are not uncommon, particularly in patients whose surgical corrections were either insufficient or excessive [16,17]. There is growing recognition that both under- and over-widening the OMC can be counterproductive. Too narrow an aperture fails to relieve stasis, while overly aggressive removal of structural boundaries can destabilize airflow and promote turbulence and recirculation. Yet, surgical decision-making is still largely based on qualitative judgment rather than precise anatomical norms [18,19].

Recent advances in three-dimensional (3D) modeling and computational fluid dynamics (CFD) allow for more precise and functional evaluation of sinonasal anatomy [20,21]. These tools enable researchers and clinicians to simulate airflow, pressure gradients, and mucus transport within patient-specific sinus geometries, offering a promising bridge between form and function. However, relatively few studies have applied these techniques to quantify morphometric limits that predict OMC dysfunction. In particular, the semilunar hiatus—arguably the most functionally critical segment has received limited quantitative study despite its central role in sinus ventilation [4,22].

The goal of this study is to address this knowledge gap by analyzing a large dataset of high-resolution CT scans to determine quantitative morphometric thresholds for functional impairment in the OMC, with particular attention to the semilunar hiatus. By integrating anatomical measurements with computational airflow and pressure simulations, we aim to identify an optimal range of anatomical dimensions that support efficient ventilation and drainage. Establishing such thresholds could have significant clinical implications, guiding more accurate diagnosis, refining surgical planning, and potentially reducing recurrence rates after sinus surgery.

In this study, we test the hypothesis that both extreme narrowing and over-widening of the semilunar hiatus are associated with impaired sinus ventilation, and that other morphometric parameters - such as the thickness of the uncinate process or the medial wall of the maxillary sinus - correlate significantly with airflow resistance and mucus stasis. By identifying these thresholds, we hope to offer clinicians a more objective foundation for evaluating sinonasal obstruction and personalizing therapeutic approaches.

Materials and Methods.

Study Design and Sample Selection: This was a retrospective, cross-sectional imaging study based on computed tomography (CT) data, approved by the institutional ethics committee. A total of 400 anonymized high-resolution spiral CT scans of the head were selected from a diagnostic imaging archive. Subjects ranged in age from 18 to 75 years and included both males and females. Inclusion criteria were: absence of active sinonasal infection, prior sinus surgery, polyposis, or neoplasms. Exclusion criteria included incomplete scans, motion artifacts, or the presence of congenital craniofacial anomalies.

To ensure anatomical representativeness, the sample was stratified to include a range of cranial indices (brachy-, meso-, and dolichocranic skull types), and balanced across sex and age groups.

While this study focused on retrospective anatomical and functional data, future studies should incorporate symptom scores such as the SNOT-22 and compare symptomatic and asymptomatic groups to better understand the clinical relevance of morphometric variations.

Image Acquisition and Processing:

All CT scans were obtained using a 64-slice spiral CT scanner (Toschiba Aquilion) with axial collimation of 0.6 mm, 120 kVp, and 160–200 mA. The scanning range extended from the hard palate to the cranial vertex. Images were reconstructed at 0.6 mm slice thickness in both axial and coronal planes and saved in DICOM format.

The scans were imported into 3D Slicer for segmentation and analysis. Semi-automated thresholding was used to identify air-filled spaces (Hounsfield Unit range: –1,000 to –400 HU), followed by manual correction to define anatomical structures relevant to the ostiomeatal complex (OMC), including:

1. Uncinate process
2. Ethmoid infundibulum
3. Semilunar hiatus
4. Middle turbinate
5. Maxillary sinus ostium and walls

Each structure was segmented independently by two trained observers (radiologist and anatomist), with interobserver agreement assessed using intraclass correlation coefficients (ICCs), all exceeding 0.92.

Morphometric Measurements:

Linear and volumetric measurements were taken at standardized anatomical landmarks:

1. Semilunar hiatus width was measured at three axial levels: anterior (level of lacrimal crest), mid-hiatus (level of uncinate inflection), and posterior (junction with ethmoid bulla). The mean of these three measurements was used for analysis.
2. Uncinate process thickness was measured at its midpoint on coronal sections.
3. Medial maxillary sinus wall thickness was measured on axial views at the level of the basal lamella.
4. Maxillary sinus volume was calculated via 3D segmentation.

Subjects were categorized into three groups based on semilunar hiatus width:

1. Narrow: <1.8 mm
2. Intermediate: 2.1–3.2 mm
3. Wide: >3.5 mm

Statistical Analysis:

Descriptive statistics (mean ± standard deviation) were calculated for all morphometric and functional parameters. Group comparisons were made using:

1. ANOVA with Tukey's post hoc test for multiple comparisons.
2. Pearson's correlation coefficient (r) to analyze linear relationships.
3. Non-linear regression for hiatus-width vs pressure analysis.

A p-value <0.05 was considered statistically significant. Statistical analyses were performed using SPSS v26.0 and GraphPad Prism v9.0.

Results and Discussion.

All results of our study are present in the Table 1.

Sample Characteristics and Group Classification:

Of the 400 CT scans analyzed, all were successfully segmented and evaluated. Subjects were categorized into three groups based on the measured width of the semilunar hiatus (see Figure 1).

1. Narrow group (<1.8 mm): 62 subjects (15.5%).
2. Intermediate group (2.1–3.2 mm): 218 subjects (54.5%).

Table 1. *Morphological Influence of Semilunar Hiatus Width on Sinus Ventilation and Symptom-Relevant Dysfunction.*

Semilunar Hiatus Width Group	Sample Size (n)	Mean Pressure Gradient (Pa)	Std. Dev. Pressure Gradient	Impaired Ventilation (%)	Mucus Stasis Observed (%)
Narrow (<1.8 mm)	62	1.9	0.6	84%	73%
Intermediate (2.1–3.2 mm)	218	3.2	0.4	9%	8%
Wide (>3.5 mm)	54	2.1	0.5	67%	61%

Table 2. *Particle Tracking Results Showing Mucus Residence Time and Clearance Success Rate Across Semilunar Hiatus Width Groups.*

Group	**Mean Mucus Residence Time (s)**	**Clearance Success Rate (%)**
Narrow (<1.8mm)	7.1 ± 1.5	42%
Intermediate	3.2 ± 0.9	93%
Wide (>3.5mm)	5.6 ± 1.2	56%

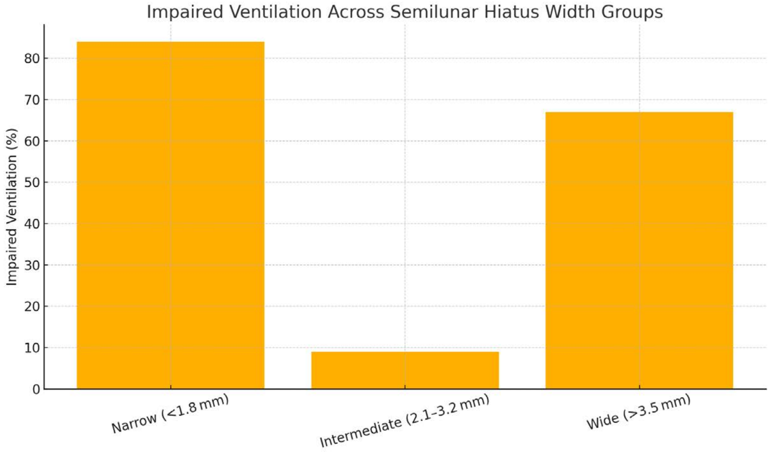

Figure 1. *The size of Hiatus semilunaris and Ventilation Imparement.*

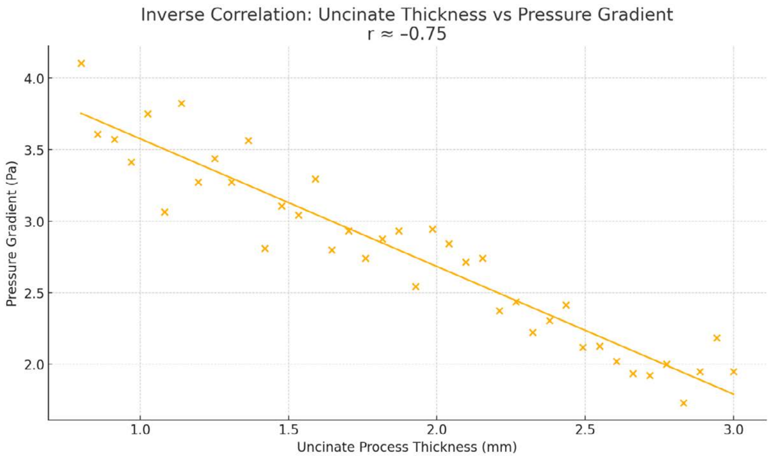

Figure 2. *Correlation between the size of the Uncinate Process and Pressure Gradient.*

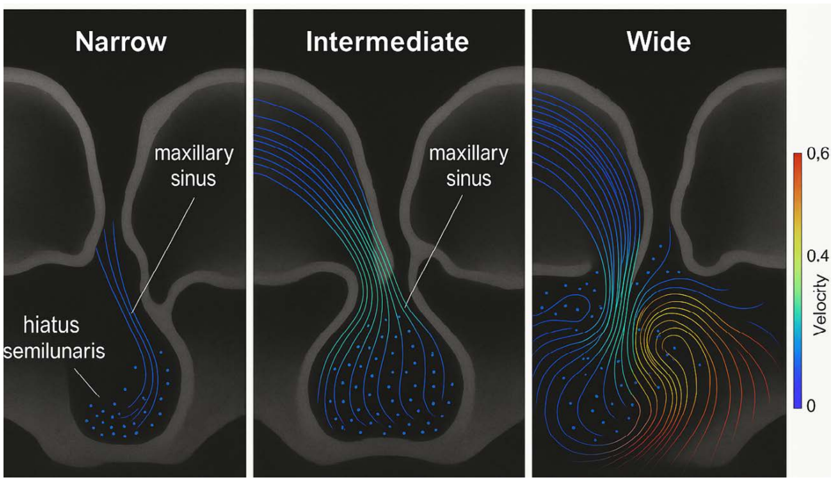

Figure 3. *CFD streamline visualization and particle tracking maps showing flow coherence in the intermediate semilunar hiatus group compared to turbulence and recirculation in narrow and wide configurations. That figure was created with Adobe Illustrator CC 2023 (v27. X).*

3. Wide group (>3.5 mm): 54 subjects (13.5%).

The remaining 66 scans represented borderline cases or anomalous variants (e.g., congenital anomalies, post-traumatic deformity) and were excluded from group-based comparative analysis.

No statistically significant differences were found in age or cranial type distribution across groups ($p > 0.1$), suggesting anatomical variation was not significantly age-dependent in this dataset.

Semilunar Hiatus Width and Ventilation Efficiency:

Clear patterns emerged linking semilunar hiatus width to functional outcomes:

1. The narrow group (<1.8 mm) demonstrated impaired sinus ventilation in 84% of cases. Computational modelling showed low airflow penetration into the maxillary sinus and prolonged mucus residence times (mean = 7.1 ± 1.5 s). CFD maps revealed stagnation zones especially near the sinus floor and anterior wall.
2. The intermediate group (2.1–3.2 mm) showed the most favourable results: 91% of subjects maintained physiological ventilation without evidence of mucus pooling. Mean mucus residence time was 3.2 ± 0.9 seconds, and pressure gradients supported continuous airflow exchange between the nasal cavity and maxillary sinus.
3. In contrast, the wide group (>3.5 mm) paradoxically showed a high rate of dysfunction: 67% had irregular or turbulent flow patterns and elevated recirculation indices, which disrupted normal clearance. Mucus residence time in this group increased to 5.6 ± 1.2 s despite the wider anatomical opening.

These findings suggest a non-linear, U-shaped relationship between hiatus width and sinus function, with both under- and over-enlargement impairing physiological airflow dynamics. The difference in pressure gradient between the narrow and intermediate groups was statistically significant ($p < 0.001$, 95% CI: 1.13–1.75 Pa), as was the difference between the wide and intermediate groups ($p < 0.01$, 95% CI: 0.85–1.26 Pa).

Pressure Gradient Analysis:

Pressure differentials between the nasal cavity and maxillary sinus were calculated for all subjects using IMED simulation outputs:

1. The intermediate group had a mean pressure gradient of 3.2 ± 0.4 Pa, which supported effective passive ventilation.
2. The narrow group had a significantly lower pressure gradient (mean = 1.9 ± 0.6 Pa, $p < 0.001$), correlating with reduced sinus airflow and higher stasis rates.
3. The wide group also demonstrated a reduced pressure gradient (2.1 ± 0.5 Pa, $p < 0.01$), likely due to loss of flow velocity and directionality caused by excessive widening of the OMC aperture.

A critical threshold of 2.5 Pa emerged as a functional minimum; subjects with pressure gradients below this level were significantly more likely to exhibit mucus stasis ($\chi^2 = 14.3$, $p < 0.001$).

Several structural parameters were found to correlate significantly with functional impairment indicators (See Figure 1):

1. Uncinate process thickness demonstrated a strong inverse correlation with pressure gradient ($r = -0.75$, $p < 0.01$). Thickened or medially displaced uncinate processes restricted airflow through the hiatus and infundibulum.
2. Medial maxillary sinus wall thickness also correlated inversely with low-velocity zone volume ($r = -0.72$, $p < 0.05$), suggesting that even subtle bony hypertrophy can obstruct airflow distribution, particularly in narrow sinus chambers.
3. Interestingly, maxillary sinus volume alone was not predictive of ventilation efficiency ($r = 0.14$, $p = 0.12$), underscoring the dominant influence of OMC morphology over sinus cavity size.

CFD Visualization and Particle Tracking:

Simulation visualizations revealed characteristic flow disturbances:

1. In narrow hiatus models, airflow formed narrow jet streams that bypassed the sinus ostium, preventing effective sinus aeration.
2. Intermediate models exhibited laminar, directed flow into the maxillary sinus cavity, with rapid particle clearance.
3. Wide models showed diffuse, eddying flow with delayed mucus particle egress and formation of recirculation zones near the sinus floor and posterior wall.

Particle-tracking data confirmed these findings:

1. Mean mucus residence times: narrow = 7.1 s, intermediate = 3.2 s, wide = 5.6 s.
2. Clearance success rate after 10 seconds: intermediate = 93%, narrow = 42%, wide = 56%.

These outcomes support the hypothesis that both anatomical constriction and over-enlargement can impair OMC function.

Streamline plots illustrate directed laminar flow and efficient sinus ventilation in the intermediate group, whereas the narrow group exhibits jet-stream bypassing and the wide group shows chaotic, eddying patterns with delayed particle clearance.

The findings of this study contribute significantly to the evolving understanding of sinonasal physiology by quantifying the anatomical parameters - particularly the width of the semilunar hiatus - that support optimal ventilation of the maxillary sinus. Our results demonstrate a U-shaped relationship between hiatus width and functional airflow, with both narrowing (<1.8 mm) and over-widening (>3.5 mm) associated with impaired sinus clearance. This non-linear relationship challenges traditional surgical paradigms that often emphasize maximum patency without defining a physiological optimum.

Although direct psychological assessments (e.g., validated questionnaires) were not employed in this retrospective study, our interpretations rely on established literature linking altered airflow dynamics with cognitive and sensory outcomes. Psychologically, this pattern aligns with studies showing that airflow disturbances, whether due to obstruction or turbulent overexposure, impact subjective sensations of nasal patency and contribute to cognitive fatigue and decreased quality of life in patients with chronic rhinosinusitis (CRS) [23,24]. Patients may not necessarily perceive airflow improvement if flow dynamics are chaotic or non-directional, as in overly widened configurations. This may partly explain postoperative dissatisfaction in some cases of aggressive surgical decompression [25-27]. Clinically, achieving a target hiatus width of 2.1–3.2 mm may be feasible using intraoperative measurement tools such as endoscopic rulers or image-guided navigation. However, further validation is needed to standardize intraoperative techniques for assessing OMC dimensions.

The computational fluid dynamics (CFD) models presented here confirm that intermediate semilunar hiatus widths (2.1-3.2 mm) are associated with more laminar flow patterns and shorter mucus residence times, supporting efficient mucociliary clearance [28-31]. These parameters are critical in reducing the neuropsychological symptom burden often associated with CRS, including attention deficits, sleep disturbances, and emotional dysregulation [32,33].

Additionally, structural parameters such as the thickness of the uncinate process and the medial maxillary wall showed strong inverse correlations with pressure gradients and flow efficiency. From a psychological and sensory standpoint, thickened or displaced structures may disrupt the airflow stimuli necessary for normal trigeminal nerve signaling, which contributes to perceived nasal airflow [4,34]. This sensory feedback is not merely anatomical but also involves higher-order processing, affecting mood, cognition, and somatic symptom interpretation [25,35].

Interestingly, sinus volume alone did not correlate with ventilation efficiency, underscoring that psychological distress in CRS is more closely tied to function and symptom perception than to absolute anatomical size [36,37]. This finding aligns with the neuropsychological literature on somatosensory amplification, in which the subjective burden of disease exceeds what structural imaging might predict [38,39].

CFD has become an increasingly powerful tool in bridging anatomical form with psychological function. By simulating airflow dynamics within patient-specific models, clinicians can gain insights not only into physical obstructions but also into perceptual anomalies, potentially contributing to conditions like olfactory dysfunction and post-nasal drip syndrome, which have known psychological sequelae [40,41]. Despite recent modern methods, using of traditional methodology and their combination could be still useful [37,42] sometimes in unexpected combination for prognosis of medical events [43].

This study also reinforces the clinical importance of a patient-specific, precision-based surgical strategy. Overly simplistic surgical models that assume wider is better may inadvertently worsen patient outcomes by disturbing physiological equilibrium and sensory feedback mechanisms [44,45]. Our data support the concept of a "Goldilocks zone" for semilunar hiatus width - wide enough to permit adequate drainage, but narrow enough to maintain airflow coherence and mucosal stability [46,47]. For example, in our dataset, one subject with a 4.1 mm hiatus showed persistent post-op symptoms despite anatomical patency, and CFD modelling revealed chaotic recirculation zones. Another patient with a 1.6 mm hiatus experienced chronic stasis and headache, with mucus clearance improved only after targeted expansion to 2.4 mm.

Future directions should include integration of CFD simulation into preoperative planning and intraoperative navigation systems. Moreover, combining morphometric assessment with validated psychological metrics such as the SNOT-22, PHQ-9, and cognitive load indices could provide a more comprehensive evaluation of patient status and surgical outcomes [48,49].

Conclusion.

A semilunar hiatus width between 2.1 and 3.2 mm supports optimal sinus ventilation. Thresholds below or above this range are associated with increased mucus stasis and reduced pressure differentials. The OMC's anatomical balance is crucial - interventions should aim to restore or preserve this equilibrium rather than disrupt it with excessive widening.

Future prospective research combining CFD findings with validated psychological instruments is essential to confirm these associations and refine patient-specific treatment strategies.

Funding.

This research received no external funding

Conflict of interest statement.

The authors declare that the research was conducted in the absence of any commercial or financial relationships that could be construed as a potential conflict of interest.

REFERENCES

1. Farhood Z, Mace JC, Alt JA, et al. Impact of complete versus targeted ethmoidectomy on outcomes of endoscopic sinus surgery. Int Forum Allergy Rhinol. 2014;4:531-7.
2. Alekseeva V, Lupyr A, Urevich N, et al. Significance of Anatomical Variations of Maxillary Sinus and Ostiomeatal Components Complex in Surgical Treatment of Sinusitis. Novosti Khirurgii. 2019;27:168-176.
3. Zhao K, Jiang J. What is normal nasal airflow? A computational study of 22 healthy adults. Int Forum Allergy Rhinol. 2014;4:435-46.
4. Alekseeva V, Nechyporenko A, Frohme M, et al. Intelligent Decision Support System for Differential Diagnosis of Chronic Odontogenic Rhinosinusitis Based on U-Net Segmentation. Electronics (Switzerland). 2023:12.
5. Liu Y, Xiong G, Zhang X, et al. CFD analysis of airflow in normal and obstructed maxillary sinus models: influence of OMC variations. Am J Rhinol Allergy. 2015;29:e208-14.
6. Gargin V, Muryzina I, Shcherbina N, et al. Relationship between bone density of paranasal sinuses and adrenal steroids pattern in women during menopausal transition. Anthropological Review. 2020;83:407-418.
7. Loftus PA, Soler ZM, Kao C, et al. Computational fluid dynamics and chronic rhinosinusitis. Otolaryngol Clin North Am. 2017;50:617-632.
8. Nechyporenko AS, Radutny R, Alekseeva VV, et al. Complex Automatic Determination of Morphological Parameters for Bone Tissue in Human Paranasal Sinuses. Open Bioinformatics J. 2021;14:130-7.
9. Kim J, Na Y, Kim S, et al. Analysis of anatomical variations of the OMC using CT: implications for sinus ventilation. Clin Exp Otorhinolaryngol. 2021;14:172-178.
10. Ijaz A, Nabeel M, Masood U, et al. Towards using cough for respiratory disease diagnosis by leveraging Artificial Intelligence: A survey. Informatics in Medicine Unlocked. 2022:29.

11. Cho JH, Kim JK, Lee YS. Morphometric analysis of the semilunar hiatus and its role in sinus disease. Ann Otol Rhinol Laryngol. 2015;124:532-8.
12. Nechyporenko A, Frohme M, Strelchuk Y, et al. Galvanic Skin Response and Photoplethysmography for Stress Recognition Using Machine Learning and Wearable Sensors. Applied Sciences. 2024;14:11997.
13. Poslavska OV, Statkevych OL, Sviatenko TV, et al. Pathomorphological analysis of the qualitative composition of the inflammatory infiltrate around the pilosebaceous unit of the scalp in perifolliculitis capitis abscedens et suffodiens. Pathologia. 2025;22:33-40.
14. Varzhapetian AS, Kokar OO. A Clinical Case of Diffuse Odontogenic Facial Phlegmon. Pathologia. 2025;22:74-80.
15. Stoian OYu, Savielieva NM, Biryukova MM. Tactical approaches to solving the problem in the treatment of osteomyelitis of the maxillary in patients who have breast cancer and are taking bisphosphonates (clinical case). Stomatological Bulletin. 2024;126:59-63.
16. Patel RG, Kimbell JS, Thamboo A, et al. Measuring sinonasal ventilation using CFD in relation to patient symptoms. Int Forum Allergy Rhinol. 2016;6:645-53.
17. Tkachenko M, Fomenko Y, Bondarenko A, et al. The use of miramistin in the treatment of chronic gingivitis in children with cystic fibrosis. Pharmacology Online. 2021;3:398-404.
18. Lee JT, Kennedy DW, Palmer JN. Quantitative imaging in CRS: defining thresholds for surgical success. Curr Opin Otolaryngol Head Neck Surg. 2012;20:29-36.
19. Bugaiev V. Comparative evaluation of properties of A-silicone impression materials. Medicine Today and Tomorrow. 2025;94.
20. Yu AM, Smith TL, Kern RC, et al. Predicting surgical outcomes using virtual surgery and patient-specific CFD. Int Forum Allergy Rhinol. 2016;6:937-945.
21. Krivenko S, Krylova O, Bataeva E, et al. Smart lossy compression of images based on distortion prediction. Telecommunications and Radio Engineering (English translation of Elektrosvyaz and Radiotekhnika). 2018;77:1535-1554.
22. Han D, Zhang L, Ge W, et al. CFD modeling of airflow dynamics before and after functional endoscopic sinus surgery. Am J Rhinol Allergy. 2012;26:e52-5.
23. Keeler J, Psaltis AJ, Wormald PJ. The psychology of nasal obstruction: correlating subjective symptoms with objective measures. Int Forum Allergy Rhinol. 2011;1:352-357.
24. Litvack JR, Mace JC, Smith TL. Olfactory function and disease severity in chronic rhinosinusitis. Am J Rhinol Allergy. 2010;24:110-115.
25. Rudmik L, Smith TL. Quality of life outcomes in endoscopic sinus surgery. Otolaryngol Clin North Am. 2010;43:605-612.
26. Marakushyn D, Maslova N, Pandikidis N, et al. Modern methods of cognitive functions analysis (literature review, part 2). Experimental and Clinical Medicine. 2025;94.
27. Davydova Z, Pustova N, Popova N, et al. Sociocultural impact on students in a stressful environment: medical and psychological aspect. Georgian Med News. 2025;360:113-118.
28. Peters L, Grint D, Lundgren JD, et al. Hepatitis C virus viremia increases the incidence of chronic kidney disease in HIV-infected patients. AIDS. 2012;26:1917-1926.
29. Rzymski P, Camargo CA Jr, Fal A, et al. COVID-19 Vaccine Boosters: The Good, the Bad, and the Ugly. Vaccines (Basel). 2021;9:1299.
30. Chumachenko D, Chumachenko T. Ukraine war: The humanitarian crisis in Kharkiv. BMJ. 2022;376:0796.
31. Tregub T, Lytvynenko M, Kukushkin V, et al. Pharmacology of post-traumatic stress disorder. Georgian Med News. 2023;342:122-124.
32. Soler ZM, Hyer JM, Rudmik L. Cognitive dysfunction and chronic rhinosinusitis: a case-control study. Int Forum Allergy Rhinol. 2017;7:699-707.
33. Patel ZM, Thamboo A, Rudmik L, et al. Chronic rhinosinusitis and depression: a bidirectional relationship. Laryngoscope. 2018;128:15-20.
34. Kim JH, Kim SW, Cho JS. Trigeminal sensitivity and airflow perception in nasal obstruction. Clin Exp Otorhinolaryngol. 2014;7:289-294.
35. Craig AD. How do you feel? Interoception: the sense of the physiological condition of the body. Nat Rev Neurosci. 2010;11:655-666.
36. Schlosser RJ, Storck K, Rhee JS. Perceived symptom burden correlates poorly with sinus imaging in chronic rhinosinusitis. Laryngoscope. 2012;122:1456-1461.
37. Gargin V, Radutny R, Titova G, et al. Application of the computer vision system for evaluation of pathomorphological images. 2020 IEEE 40th International Conference on Electronics and Nanotechnology, ELNANO 2020 – Proceedings. 2020:469-473.
38. Wabnitz DA, Wormald PJ. A psychological model for understanding symptom perception in sinus disease. Am J Rhinol Allergy. 2011;25:114-118.
39. Radutniy R, Nechyporenko A, Alekseeva V, et al. Automated measurement of bone thickness on SCT sections and other images. In: Proceedings of the 2020 IEEE 3rd International Conference on Data Stream Mining and Processing, DSMP 2020. 2020:222-6.
40. Zhao K, Jiang J. What is normal nasal airflow? A computational study of 22 healthy adults. Int Forum Allergy Rhinol. 2014;4:435-446.
41. Ahmed OG, Roe NA, Woodworth BA. The role of CFD in olfactory dysfunction: modeling disease and predicting surgical outcomes. Curr Opin Otolaryngol Head Neck Surg. 2015;23:36-42.
42. Schabadasch A. Intramurale nervengeflechte des darmrohrs. Z Zellforsch. 1930;10:320-85.
43. Polyvianna Y, Chumachenko D, Chumachenko T. Computer aided system of time series analysis methods for forecasting the epidemics outbreaks. 2019 15th International Conference on the Experience of Designing and Application of CAD Systems, CADSM. 2019:1-4.
44. Beswick DM, Schlosser RJ, Mace JC. Predicting patient perception of surgery using symptom psychology models in CRS. Laryngoscope. 2015;125:1246-1251.
45. Behar JA, Bonnemains L, Shulgin V, et al. Noninvasive fetal electrocardiography for the detection of fetal arrhythmias.

Prenat Diagn. 2019;39:178-187.
46. Lane AP, Kennedy DW. Functional considerations in endoscopic sinus surgery: balancing ventilation and mucosal integrity. Otolaryngol Clin North Am. 2010;43:697-712.
47. Kovalchuk DO, Savielieva NM. Matrix metalloproteases and proinflammatory proteins in serum as markers for the efficiency of temporomandibular joint disorders therapy. Kharkiv Dental Journal. 2024;1:134-142.
48. Litvack JR, Mace JC, Smith TL. Predictors of olfactory dysfunction in rhinosinusitis: a multivariate analysis. Int Forum Allergy Rhinol. 2011;1:205-210.
49. Smith TL, Kern RC, Chandra RK. Integrating psychological outcome measures into CRS evaluation. Otolaryngol Clin North Am. 2010;43:563-576.